chemistry

MDPI

Article

Head vs. Tail Squaramide–Naphthalimide Conjugates: Self-Assembly and Anion Binding Behaviour

Anthony A. Abogunrin [1], Stephen A. Healy [1], Orla Fenelon [1] and Robert B. P. Elmes [1,2,3,*]

[1] Department of Chemistry, Maynooth University, National University of Ireland, Co. Kildare, W23 F2H6 Maynooth, Ireland
[2] Synthesis and Solid State Pharmaceutical Centre (SSPC), University of Limerick, V94 T9PX Limerick, Ireland
[3] Kathleen Lonsdale Institute for Human Health Research, Maynooth University, National University of Ireland, Co. Kildare, W23 F2H6 Maynooth, Ireland
* Correspondence: robert.elmes@mu.ie; Tel.: +353-1-7084615

Abstract: The syntheses of two squaramide–naphthalimide conjugates (**SN1** and **SN2**) are reported; the structures of **SN1** and **SN2** differ by the attachment of a squaramide—either at the 'head' or the 'tail' of the naphthalimide fluorophore. Both compounds displayed weak fluorescence due to the inclusion of a nitro-aromatic squaramide which efficiently quenches the emission of the naphthalimide. Both compounds were also shown to undergo self-aggregation as studied by ^{1}H NMR and scanning electron microscopy (SEM). Furthermore, **SN1** and **SN2** gave rise to stark colourimetric changes in response to basic anions such as AcO^-, SO_4^{2-} HPO_4^{2-}, and F^-. The observed colour changes are thought to be due to deprotonation of a squaramide NH. The same basic anions also result in a further quenching of the naphthalimide emission. No colour change or emission modulations were observed in the presence of Cl^-; however, ^{1}H NMR studies suggest that moderate H-bonding occurs between this anion and both **SN1** and **SN2**.

Keywords: supramolecular chemistry; squaramide; 1,8-naphthalimide; sensor; anion recognition; aggregation

Citation: Abogunrin, A.A.; Healy, S.A.; Fenelon, O.; Elmes, R.B.P. Head vs. Tail Squaramide–Naphthalimide Conjugates: Self-Assembly and Anion Binding Behaviour. *Chemistry* **2022**, *4*, 1288–1299. https://doi.org/10.3390/chemistry4040085

Academic Editor: Xin Wu

Received: 24 August 2022
Accepted: 5 October 2022
Published: 18 October 2022

1. Introduction

Squaramides have attracted a significant amount of research attention in recent years due to several physical and chemical characteristics that render them an ideal scaffold on which to build charge neutral anion receptors [1,2]. Their ability to partake in bi-directional H-bonding that increases the aromatic character of the cyclobutenedione ring [3,4] has been seen to be of particular benefit for the recognition of halides [5–8]. Indeed, Amendola et al. showed that a simple squaramide-based receptor forms 1:1 complexes with halide ions that are up to 2 orders of magnitude more stable than the corresponding urea-based receptor [9]. This finding has led to several examples of their exploitation as anion transporters [10–13] with the ability to disrupt anion homeostasis in cellular models whereby the transport ability of the receptors leads to apoptosis and induced autophagy [14,15]. In parallel, the 1,8-naphthalimide fluorophore has also found significant use in the construction of anion sensors whereby the ICT character of the naphthalimides can be modulated upon interaction with anionic species [16]. Gunnlaugsson et al. pioneered their use in this area where they reported a series of studies on naphthalimide–urea conjugates [17–23].

Our interest in anion recognition and sensing has centred on the squaramide motif where the aforementioned bidirectional H-bonding interactions in addition to π–π stacking brought about by the aromatic cyclobutenedione ring give a useful handle on which to build effective anion sensors [24–31]. We recently reported a series of naphthalimide–squaramide conjugates that aggregated in solution and were capable of sensitive detection of bromide through an 'aggregation–disggregation approach' [32]. The aggregation behaviour of these conjugates could be modulated upon bromide recognition where the disruption of

H-bonding reversed self-assembly and gave rise to a 'switch on' fluorescence response. In the current work, we have designed and synthesised a further set of squaramide–naphthalimide conjugates in which we have changed the functionality of the phenyl substituent of the squaramide. Again, we have placed the squaramide at either the 'head' or the 'tail' of the naphthalimide. We envisioned that the inclusion of a nitro group in the structures would provide a stronger H-bonding receptor while also providing interesting photophysical properties to the conjugates.

Herein, we report the synthesis of compounds **SN1** and **SN2** (Figure 1) and carry out an investigation on both their aggregation behaviour and their anion recognition properties.

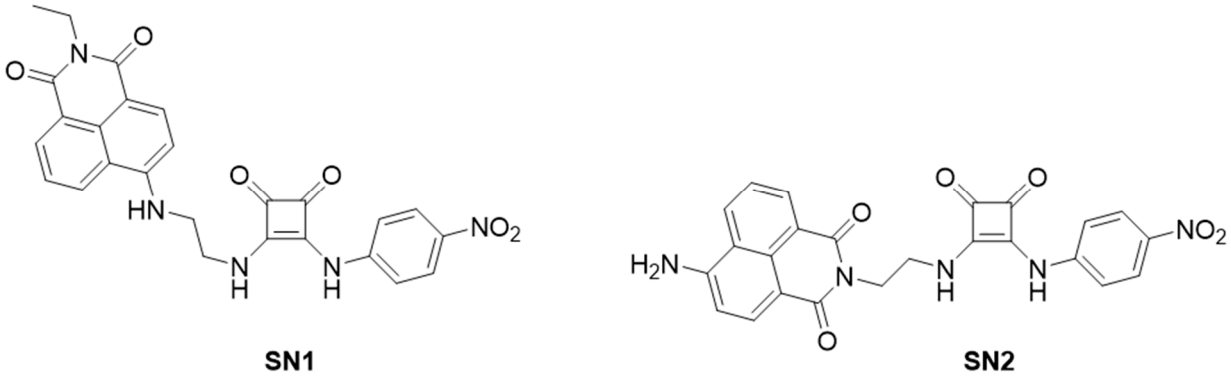

Figure 1. Chemical structures of probes **SN1** and **SN2**.

2. Materials and Methods

General Experimental Methods

All chemicals purchased were obtained from commercial suppliers and used without further purification. DCM was distilled over CaH_2 and MeCN was dried over 3 Å molecular sieves. Anhydrous DMF was purchased from Sigma Aldrich (Arklow, Ireland). TLC was performed on Merck Silica Gel F254 plates (Merck Life Science Limited, Cork, Ireland) and visualised under UV light (λ = 254 nm). Flash chromatography was performed with Merck Silica Gel 60 (Merck Life Science Limited, Ireland). Compounds were lyophilised on a Labconco Freezone 1 Dry system. NMR spectra were recorded on a Bruker Ascend 500 NMR spectrometer, operated at 500 MHz for ^{1}H NMR analysis and 126 MHz for ^{13}C analysis, both at 293 and 343 K. The residual solvent peak was used as an internal standard for DMSO-d_6 and TMS for $CDCl_3$. Chemical shifts (δ) were reported in ppm. NMR spectra were processed and stack plots produced using MestReNova 6.0.2 software. Proton and carbon signals were assigned with the aid of 2D NMR experiments (COSY, HSQC, and HMBC). Multiplicity is given as s = singlet, bs = broad singlet, d = doublet, brd = broad doublet, dd = doublet of doublets, ddd = doublet of doublet of doublets, t = triplet, q = quartet, m = multiplet as appropriate, and J values are given in Hz. Infrared spectra were obtained via ATR as a solid on a zinc selenide crystal in the region of 4000–400 cm^{-1} on a Perkin Elmer Spectrum 100 FT-IR spectrophotometer. LC-MS was performed on an Agilent Technologies 1200 Series instrument consisting of a G1322A Quaternary pump and a G1314B UV detector (254 nm) coupled to an Advion Expression L Compact Mass spectrometer (ESI) operating in positive mode. High-resolution ESI spectra were recorded on an Agilent 6310 LCMS TOF. UV/Vis spectra were recorded on a Varian Cary 50 Scan UV/Vis spectrophotometer and fluorescence spectra were measured using a Cary Eclipse operating Cary WinUV software. Diethyl squarate was synthesised as previously described [33].

6-((2-Aminoethyl)amino)-2-ethyl-1H-benzo[de]isoquinoline-1,3(2H)-dione (2)

A solution of **1** (1 g, 3.29 mmol, 1 eq.) was stirred at room temperature overnight in neat ethylenediamine (10 mL, excess) to yield a dark orange liquid. The crude product was slowly added to deionised water (50 mL) and left to stir at room temperature for

2 h. The precipitate was collected by suction filtration and washed with H_2O to yield the product as a yellow amorphous solid (0.75g, 80%). ^{1}H NMR, (DMSO-d_6, 500.13 MHz) δ (ppm), *J* (Hz): 8.63 (dd, *J* = 8.4, *J* = 0.8, 1H, ArH), 8.36 (dd, *J* = 7.3, *J* = 0.9, 1H, ArH), 8.18 (d, *J* = 8.5, 1H, ArH), 7.60 (m, 1H, ArH), 6.73 (d, *J* = 8.5, 1H, ArH), 3.97 (q, *J* = 6.4, 2H, CH_2), 3.32 (t, *J* = 6.4, 2H, CH_2), 2.82 (t, *J* = 6.4, 2H, CH_2), 1.11 (t, *J* = 7.0, 3H, CH_3); ^{13}C NMR, (DMSO-d_6, 125.76 MHz) δ (ppm): 164.0, 163.1, 151.3, 134.6, 131.0, 129.8, 129.0, 124.6, 122.3, 120.6, 108.1, 104.3, 46.7, 34.7, 13.7; HRMS (ESI) calcd. for $C_{16}H_{18}N_3O_2$ $[M + H]^+$ 284.1394, found 284.1389; difference −1.65 ppm; ν_{max} (KBr)/cm^{-1}: 3358 (N-H), 2979 (ArH), 1676 (C=O), 1461 (ArH), 1370 (CH), 1249 (C-N).

3-Ethoxy-4-((4-nitrophenyl)amino)cyclobut-3-ene-1,2-dione (3)

A solution of 4-nitroaniline (1.63 g, 11.75 mmol, 1 eq.) in EtOH (5mL) was slowly added to a mixture of diethyl squarate (1.74 mL, 11.75 mmol, 1 eq.) and zinc triflate (0.85 g, 2.35 mmol, 0.2 eq.) in EtOH (5 mL). The reaction was stirred at room temperature overnight. The precipitate was collected by suction filtration and washed with EtOH and Et_2O to yield the product as an orange amorphous solid (2.901g, 94%). *1*H NMR, (DMSO-d_6, 500.13 MHz) δ (ppm), *J* (Hz): 11.22 (s, 1H, NH), 8.24 (d, *J* = 9.0, 2H, ArH), 7.59 (d, emphJ = 9.0, 2H, ArH), 4.80 (q, *J* = 7.1, 2H, CH_2), 1.44 (t, *J* = 7.1, 3H, CH_3); ^{13}C NMR (DMSO-d_6, 125.76 MHz): δ (ppm): 185.25, 169.90, 142.97, 126.87, 125.75, 119.51, 70.66, 16.06; HRMS (ESI) calcd. for $C_{12}H_{10}N_2NaO5$ $[M + Na]^+$ 285.0482, found 285.0496; difference 4.84 ppm; ν_{max} (KBr)/cm^{-1}: 3304 (N-H), 3083 (ArH), 1715 (C=O), 1623 (ArH), 1531 (N-O), 1114 (C-O).

2-Ethyl-6-((2-((2-((4-nitrophenyl)amino)-3,4-dioxocyclobut-1-en-1l)amino)ethyl)amino) -1H-benzo[de]isoquinoline-1,3(2H)-dione (SN1)

A solution of **3** (0.324 g, 1.235 mmol, 1 eq.) in EtOH (8 mL) was slowly added to a mixture of **2** (0.35 g, 1.235 mmol, 1 eq.) and Et3N (0.689 mL, 4.94 mmol, 4 eq.) in EtOH (12 mL). The reaction was stirred at room temperature. The precipitate was collected by suction filtration and washed with EtOH and Et_2O to yield the product as an orange amorphous solid (0.453 -g, 73%). ^{1}H NMR at 343K, (DMSO-d_6, 500.13 MHz) δ (ppm), *J* (Hz): 9.87 (br, 1H, NH), 8.60 (d, *J* = 8.3, 1H, ArH), 8.42 (d, *J* = 7.2, 1H, ArH), 8.26 (d, *J* = 8.5, 1H, ArH), 8.07 (brs, 2H, ArH), 7.67 (d, *J* = 8.1, 2H, ArH), 7.64 (d, *J* = 10.7, 1H, ArH), 7.38 (br, 2H, NH), 6.91 (d, *J* = 8.5, 1H, ArH), 4.03 (q, *J* = 7.0, 2H, CH_2), 3.96 (t, *J* = 6.0, 2H, CH_2), 3.70, (q, *J* = 6.0, 2H, CH_2), 1.18 (t, *J* = 7.1, 3H, CH_3); ^{13}C NMR at 343K, (DMSO-d_6, 125.76 MHz) δ (ppm): 181.3, 163.9, 163.1, 150.8, 134.2, 130.9, 129.8, 128.7, 125.6, 124.8, 122.6, 120.9, 118.1, 109.1, 104.7, 56.5, 44.2, 43.1, 34.6, 18.9, 13.6; HRMS (ESI) calcd. for $C_{26}H_{22}N_5O_6$ $[M + H]^+$ 500.1565, found 500.1557; difference −1.6 ppm; ν_{max} (KBr)/cm^{-1}: 3421 (NH), 3080 (ArH), 1797 (C=O), 1507 (N-O), 1419 (ArH), 1332 (N-O), 1246 (C-N).

Tert-butyl(2-(6-nitro-1,3-dioxo-1H-benzo[de]isoquinolin-2(3H)-yl)ethyl)carbamate (5)

Tert-butyl(2-aminoethyl)carbamate, (0.565 mL, 3.54 mmol, 1 eq.) was slowly added dropwise to a solution of **4** (0.86 g, 3.54 mmol, 1 eq.) in EtOH (20 mL). The reaction mixture was left to react in a 35 mL microwave tube for 1 hour at 110 °C, 1 mbar, and 300 watts. The precipitate was collected by suction filtration and washed with EtOH and Et_2O to yield the product as a peach amorphous solid (1.047g, 76%). ^{1}H NMR (500 MHz, DMSO-d_6) δ 8.70 (d, *J* = 8.6 Hz, 1H, ArH), 8.63 (d, *J* = 7.2 Hz, 1H, ArH), 8.60 (d, *J* = 8.0 Hz, 1H, ArH), 8.55 (d, *J* = 8.0 Hz, 1H, ArH), 8.10 (dd, *J* = 8.6, 7.4 Hz, 1H, ArH), 6.89 (t, *J* = 6.2 Hz, 1H, NH), 4.14 (t, *J* = 5.8 Hz, 2H, CH_2), 3.28 (d, *J* = 5.5 Hz, 2H, CH_2), 1.20 (s, 9H, CH_3).; ^{13}C NMR (DMSO-d_6, 125.76 MHz): δ (ppm): 163.6, 162.8, 156.2, 149.5, 132.0, 130.5, 129.9, 129.0, 128.9, 127.3, 124.6, 123.5, 123.1, 77.9, 38.0, 28.5; HRMS (ESI) calcd. for $C_{38}H_{38}N_6NaO_{12}$ $[2M + Na]^+$ 794.2471, found 794.2493; difference 2.8 ppm; ν_{max} (KBr)/cm^{-1}: 3401 (N-H), 2977 (ArH), 1714 (C=O), 1593 (ArH), 1523 (N-O), 1365 (C-H), 1192 (C-N).

2-(2-Aminoethyl)-6-nitro-1H-benzo[de]isoquinoline-1,3(2H)-dione (6)

Compound **5** (1.02 g, 2.647 mmol, 1 eq.) was dissolved in TFA:DCM (50:50) (6 mL) and was stirred at room temperature overnight. The solvent was removed under reduced

pressure to yield a beige amorphous solid (0.70 g, 93%). ^{1}H NMR (500 MHz, DMSO-d_6) δ 8.75 (dd, *J* = 8.7, 0.8 Hz, 1H, ArH), 8.67 (dd, *J* = 7.3, 0.8 Hz, 1H, ArH), 8.64 (d, *J* = 8.0 Hz, 1H, ArH), 8.59 (d, *J* = 8.0 Hz, 1H), 8.13 (dd, *J* = 8.6, 7.4 Hz, 1H), 7.81 (s, 2H, NH_2), 4.33 (t, *J* = 5.9 Hz, 2H, CH_2), 3.18 (dd, *J* = 11.2, 5.6 Hz, 2H, CH_2).; ^{13}C NMR (DMSO-d6, 125.76 MHz): δ (ppm): 164.0, 163.3, 149.7, 132.2, 130.6, 130.1, 129.4, 128.9, 127.2, 124.7, 123.4, 123.2, 38.2, 37.9; HRMS (ESI) calcd. for $C_{14}H_{12}N_3O_4$ $[M + H]^+$ 286.0822, found 286.0800; difference −7.88 ppm; ν_{max} (KBr)/cm^{-1}: 3078 (ArH), 1712 (C=O), 1595 (ArH), 1525 (N-O), 1437 (C-H), 1247 (C-N).

6-Amino-2-(2-aminoethyl)-1H-benzo[de]isoquinoline-1,3(2H)-dione (7)

Pd/C (approx. 0.2 g) was added to a solution of **6** (1.00 g, 3.50 mmol) dissolved in MeOH (40 mL). The reaction was placed under a H_2 atmosphere and left to stir at room temperature for 3 h. The reaction was filtered through a pad of celite and washed with excess MeOH; the filtrate was removed under reduced pressure to yield a mustard amorphous solid (0.673 g, 75%). 1H NMR, (DMSO-d_6, 500.13 MHz) δ (ppm), *J* (Hz): 8.63 (dd, *J* = 8.4, J = 1.1, 1H, ArH), 8.44 (dd, *J* = 7.3, *J* = 1.05, 1H, ArH), 8.21, (d, *J* = 8.4, 1H, ArH), 7.77, (br, 2H, NH_2), 7.67 (m, 1H, ArH), 7.48 (s, 2H, NH_2), 6.86 (d, *J* = 8.4, 1H, ArH), 4.27 (t, *J* = 6.0, 2H, CH_2), 3.12 (m, 2H, CH_2); ^{13}C NMR, (DMSO-d6, 125.76 MHz) δ (ppm): 164.9, 163.9, 153.3, 134.5, 131.5, 130.4, 129.9, 124.4, 122.4, 119.8, 108.6, 108.0, 38.4, 37.6; HRMS (ESI) calcd. for $C_{14}H_{13}N_3NaO_2$ $[M + Na]^+$ 279.0930, found 279.0914; difference −5.68 ppm; ν_{max} (KBr)/cm^{-1}: 3419 (N-H), 3362 (N-H), 3017 (ArH), 1636 (NH), 1485 (ArH), 1429 (C-H), 1247 (C-N).

6-Amino-2-(2-((2-((4-nitrophenyl)amino)-3,4-dioxocyclobut-1-en-1-yl)amino)ethyl)-1H-benzo[de]isoquinoline-1,3(2H)-dione (SN2)

A solution of **3** (0.1 g, 0.39 mmol, 1 eq.) in EtOH (8 mL) was slowly added to a mixture of **7** (0.1 g, 0.39 mmol, 1 eq.) and Et3N (0.217 mL, 1.56 mmol, 4 eq.) in EtOH (10 mL). The reaction was stirred at room temperature overnight. The precipitate was collected by suction filtration and washed with EtOH and Et_2O to yield the product as an orange amorphous solid (0.124g, 67%). ^{1}H NMR (500 MHz, DMSO-d_6) δ 9.66 (s, 1H), 8.60 (d, *J* = 8.4 Hz, 1H), 8.41 (d, *J* = 6.9 Hz, 1H), 8.18 (d, *J* = 8.3 Hz, 1H), 8.09 (d, *J* = 8.6 Hz, 2H), 7.64–7.57 (m, 1H), 7.40 (s, 2H), 7.23 (s, 2H), 6.85 (d, *J* = 8.4 Hz, 1H), 4.33 (t, *J* = 5.7 Hz, 2H), 3.93 (t, *J* = 5.2 Hz, 2H).). ^{13}C NMR at 343K, (DMSO-d_6, 125.76 MHz) δ (ppm): 181.3, 171.5, 164.6, 163.6, 162.6, 153.2, 145.7, 142.0, 134.3, 131.4, 130.3, 129.0, 125.7, 125.4, 124.3, 122.3, 120.0, 118.1, 108.7, 108.2, 43.0, 16.0; (although not symmetrical, the squaramide 13C signals appeared as coincident in this spectrum); HRMS (ESI) calcd. for C24H18N5O6 $[M + H]^+$ 472.1252, found 472.1248; difference −0.79 ppm; ν_{max} (KBr)/cm^{-1}: 3361 (N-H), 3250 (N-H), 1796 (C=O), 1622 (N-H), 1504 (N-O), 1432 (ArH), 1368 (C-H), 1328 (N-O), 1247 (C-N).

3. Results and Discussion

3.1. Synthesis

The syntheses of compounds **SN1** and **SN2** were achieved through an analogous method previously reported by us (Scheme 1) [32]. For **SN1**, 4-bromo-1,8-naphthalimide **1** was reacted with ethylenediamine before nucleophilic addition of the product **2** to 4-nitrophenyl squarate monoester **3** to yield **SN1** in 73% yield. Similarly, **SN2** was synthesised by reaction of 4-nitro-1,8-naphthalic anhydride **4** with *N*-Boc-ethylenediamine to give product **5**. Following TFA-mediated deprotection and reduction in the presence of H_2 and Pd/C, compound **7** was reacted with **3** to yield **SN2** in 67% yield. All compounds and intermediates were fully characterised by ^{1}H NMR, ^{13}C NMR, HRMS, and IR spectroscopy (see Supplementary Materials).

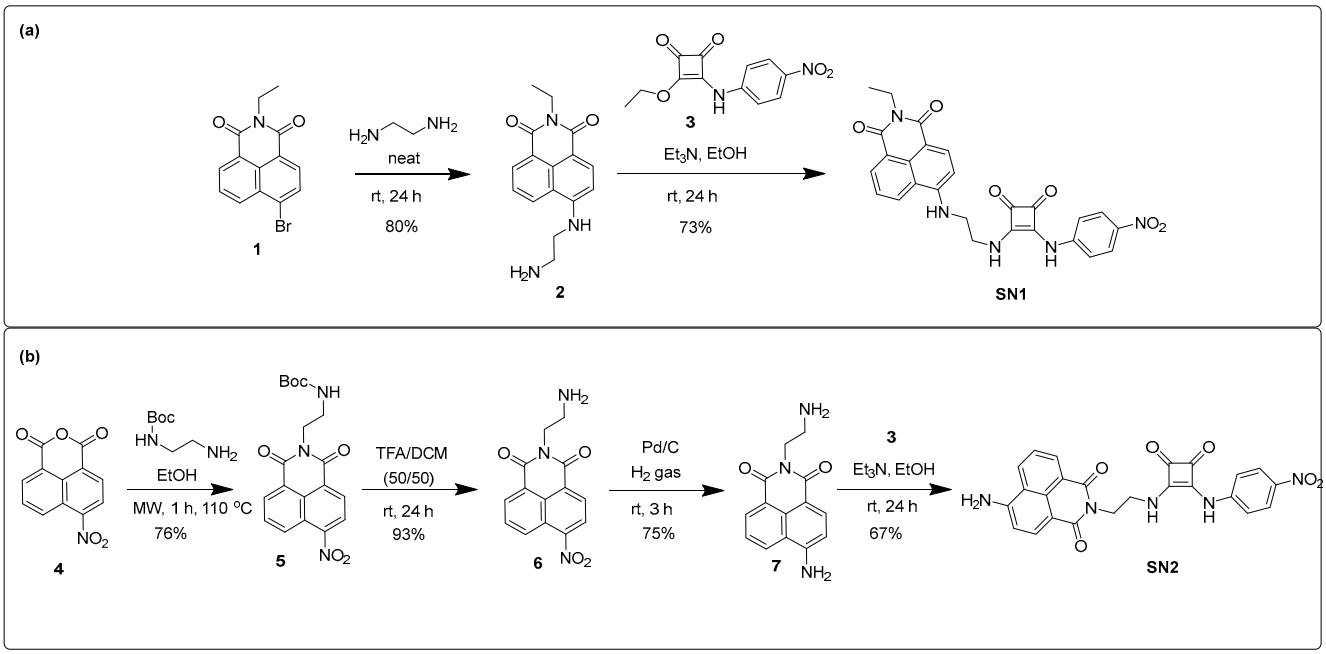

Scheme 1. Syntheses of (**a**) **SN1** and (**b**) **SN2**.

We have previously noted that the ^{1}H NMR spectra of analogous squaramide–naphthalimide conjugates give rise to complex NMR spectra showing a large degree of peak broadening owing to self-aggregation in solution. In order to investigate whether similar behaviour would be observed for **SN1** and **SN2**, ^{1}H NMR and UV/Vis absorption measurements were carried out in addition to SEM analysis.

3.2. Variable-Temperature NMR and SEM Analysis

The ^{1}H NMR spectra of **SN1** and **SN2** in DMSO-d_6 were measured at both 298 K and 343 K. There were clear differences observed between both spectra where at 298 K signals are broadened, suggesting that aggregation is occurring under these conditions. Conversely, at 343 K some signals become less broad and show a much-improved resolution while others become more broadened. Figure 2 shows the ^{1}H NMR spectrum of **SN1** at 298 K and 343 K as an example. Naphthalimide signals appear to resolve from broad to sharp for each proton while the signals associated with the 4-nitrophenyl portion display the opposite behaviour—the signal at 8.2 ppm becomes broad at 343 K and shifts upfield to 8.05 ppm while the signal at 7.45 ppm also becomes broad and shifts upfield to 7.4 ppm. Similarly, the CH_2 signals in the aliphatic region resolve from broad to sharp, clearly showing the correct multiplicity. The observation of peak broadening for the nitro-phenyl substituent suggests that this portion of the molecule is undergoing rapid rotation around the C-N bond axis at elevated temperature. This behaviour is reminiscent of a molecular rotor [34] and explains the observed peak broadening at elevated temperature. Conversely, the resolution of the CH_2 signals suggests that this linker is also taking part in the self-assembly behaviour. The broad to sharp signal resolution signifies the disaggregation event. Taken together, the evidence from the above study suggests a temperature-dependent aggregation of the molecule that involves predominantly contributions from the naphthalimide and squaramide portions of the assembly.

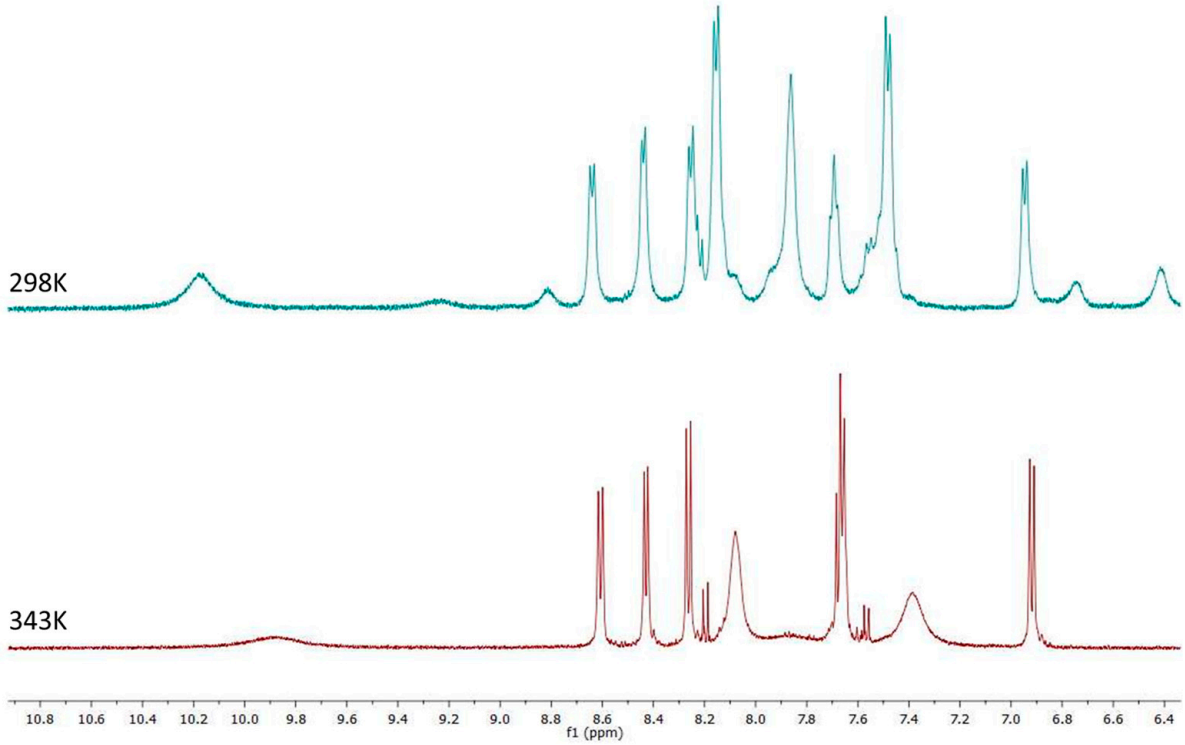

Figure 2. Variable-temperature ^{1}H NMR experiments of **SN1** at different temperatures in DMSO-d_6 (10^{-3} M).

To further probe the aggregation characteristics of both compounds, attempts were made to grow crystals from concentrated DMSO solutions. Unfortunately, in our hands the compounds did not crystallise and instead formed what appeared to be amorphous solids. The morphological features of these solids were thus analysed by scanning electron microscopy (SEM), and as shown in Figure 3, the SEM images exhibit interesting and distinct morphology on the nanoscale. **SN1** appeared as an amorphous solid with no defined structure to speak of. Conversely, **SN2** formed a porous sponge-like structure with a large degree of uniformity throughout the material. At higher magnifications, the material appeared to be composed of small 'nanoflake' type material. Although firm conclusions cannot be drawn on the exact material properties from these results, it is worth noting the difference in morphology brought about by the position of the 4-nitrophenyl-squaramide moiety, i.e., whether it is positioned at the head or the tail of the 1,8-naphthalimide. This behaviour was also seen with the 3,5-bis(trifluoromethyl)phenyl derivatives where this minor structural change gave rise to a significant change in material morphology as determined using SEM.

Both **SN1** and **SN2** were also examined using UV/Vis spectroscopy and fluorescence emission spectroscopy. The UV/Vis absorption spectrum of **SN1** in DMSO showed two absorption maxima at 280 nm and 420 nm with extinction coefficient values of 34,375 M^{-1} and 29,900 M^{-1}, respectively. Similarly, **SN2** showed an almost identical spectrum to **SN1** with maxima also at 280 nm and 420 nm and with extinction coefficients of 35,187 M^{-1} and 27,410 M^{-1}, respectively. Interestingly, a third absorption maximum at 545 nm was observed in the case of **SN2** attributed to a naphthalimide π–π stacking band (Figure 4) [35]. This peak was shown not to obey the Beer–Lambert law and further confirms the presence of a self-association event at higher concentrations of **SN2**. This behaviour was not observed for **SN1** and exemplifies the sensitivity of squaramide–naphthalimide conjugates to changes in molecular structure when considering their aggregation characteristics. A summary of the absorption properties of **SN1** and **SN2** as well as their molar absorptivities is given in Table S1.

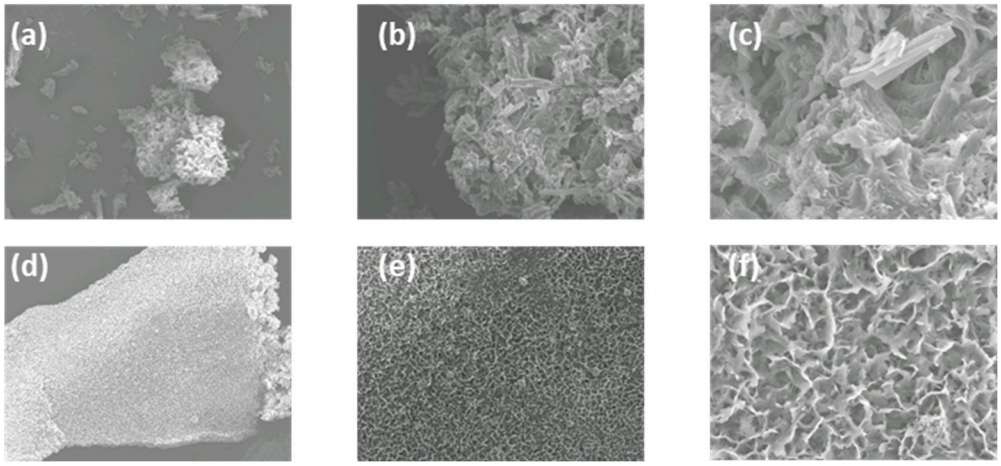

Figure 3. Scanning electron microscopy (SEM) images of the aggregates formed by self-assembly of (**a**–**c**) **SN1** and (**d**–**f**) **SN2**.

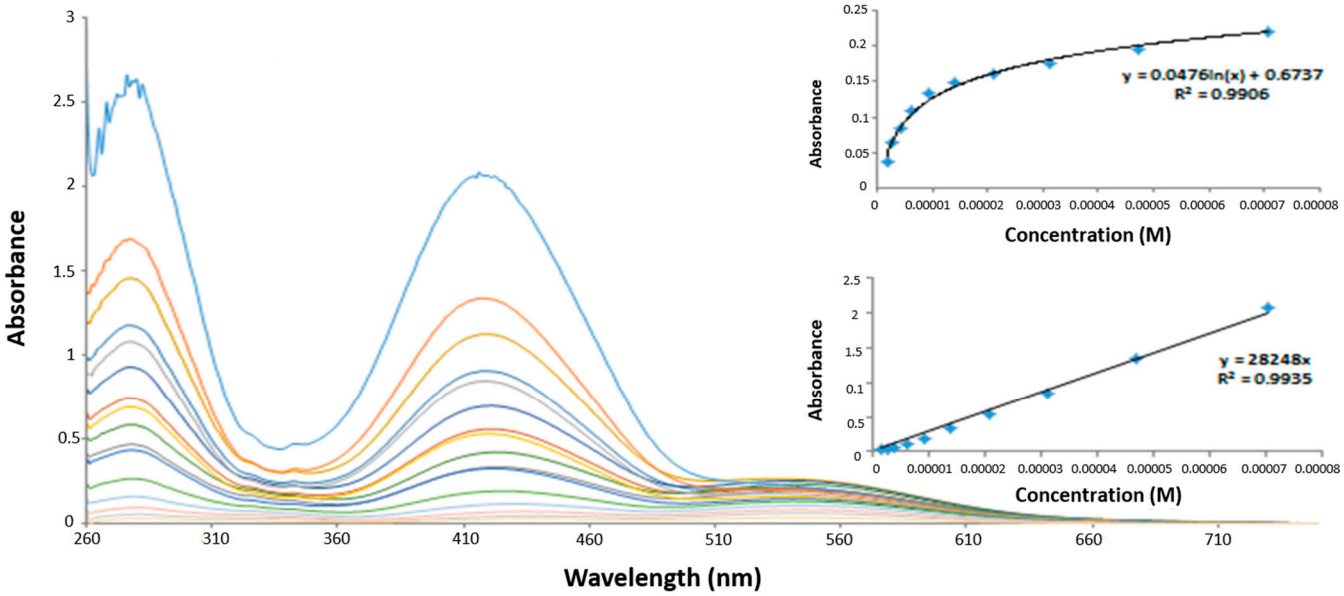

Figure 4. Changes in UV/Vis spectrum of **SN2** upon increasing concentration in DMSO (0.1–70 μM). Insets: Plots of absorbance at 420 nm and 545 nm as a function of increasing concentration of **SN2**.

Furthermore, both compounds exhibited very weak fluorescence emission at ca. 525 nm. With the aggregation behaviour observed for the previously reported analogues containing a 3,5-bis CF_3 substituent, we also undertook a thermal study to investigate if the fluorescence of **SN1** could be modulated by disaggregation. In this case, the fluorescence of **SN1** is already significantly quenched due to the inclusion of a NO_2 group which is known to efficiently quench emission from aromatic systems, including naphthalimides [36,37]. A temperature-dependent fluorescence study was undertaken in 5% aq. DMSO ranging from 298 K to 343 K where the fluorescence of both compounds was largely unaffected by temperature (see Supplementary Materials). The ^{1}H NMR results above suggest that **SN1** and **SN2** aggregate in solution but, upon heating, disassemble; however, this process cannot be monitored with fluorescence emission spectroscopy.

With the known propensity of squaramides to bind strongly to halides and other anionic species [9,10,38–42], we expected that **SN1** and **SN2** may also be capable of anion recognition and that this process may be monitored by both UV spectroscopy and ^{1}H NMR spectroscopy.

3.3. Anion Recognition

To investigate the ability **SN1** and **SN2** to bind anions in solution, a series of ^{1}H NMR experiments were carried out. Initial qualitative measurements were undertaken using a screening experiment in which 30 equivalents. of several anions (AcO^-, HPO_4^{2-}, SO_4^{2-}, F^-, and Cl^- as their tetrabutylammonium salts) were added to the receptors in solution (0.5% H_2O in DMSO-d_6). These preliminary results showed significant changes to the spectra of both **SN1** and **SN2**, where the addition of AcO^-, F^-, HPO_4^{2-}, and SO_4^{2-} led to the disappearance of the NH signal. This change was also coupled with a stark colour change from yellow to purple (or yellow to orange for SO_4^{2-}) in the cases of both receptors (see Figure 5 for **SN2**).

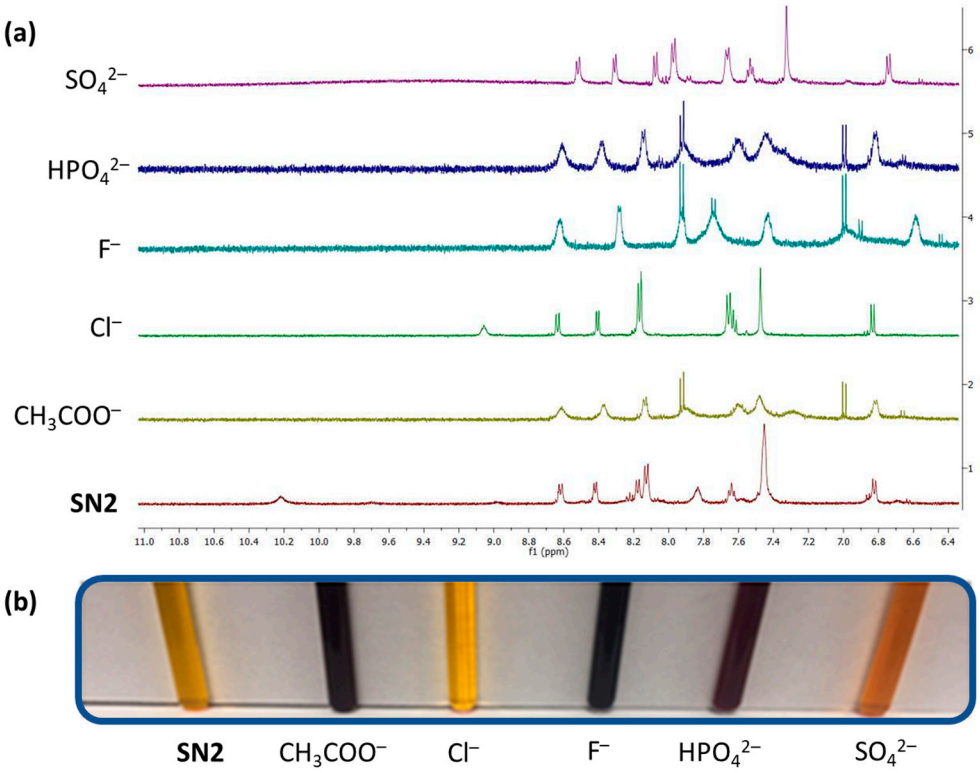

Figure 5. (**a**) ^{1}H NMR stackplot of **SN2** with various anions (30 equivalents) in 0.5% H_2O in DMSO-d_6 at 298 K. (**b**) The corresponding colour changes upon anion addition.

The disappearance of the NH signal and the colour change suggest that deprotonation of the squaramide/naphthalimide may be responsible, as has been previously observed [32]. We further confirmed this deprotonation behaviour by observation of bifluoride (HF_2^-) in the ^{1}H NMR spectra of **SN1** and **SN2** upon the addition of F^-. In comparison, the changes upon the addition of Cl^- were more subtle. For example, with **SN2,** Cl^- led to a large downfield shift of the NH signal (H_a) from 10.15 ppm to 11.5 ppm coupled with a significantly sharpened spectrum. The large downfield shift of the NH signal suggests a classical H-bonding interaction between Cl^- and the NH protons of the squaramides. More detailed ^{1}H NMR spectroscopic titrations were carried out with Cl^-, and the resulting data fit to a 1:1 binding model using the open access BindFit software program [43–45] to provide the apparent stability constants (K_a). K_a values of 273.7 M^{-1} (±4.1%) and 114.8 M^{-1} (±5.9%) were measured for receptors **SN1** and **SN2**, respectively, in DMSO-d_6 at 273 K. Figure 6 shows the changes observed in the ^{1}H NMR spectrum of **SN2** upon the addition of Cl^- (20 equivalents.).

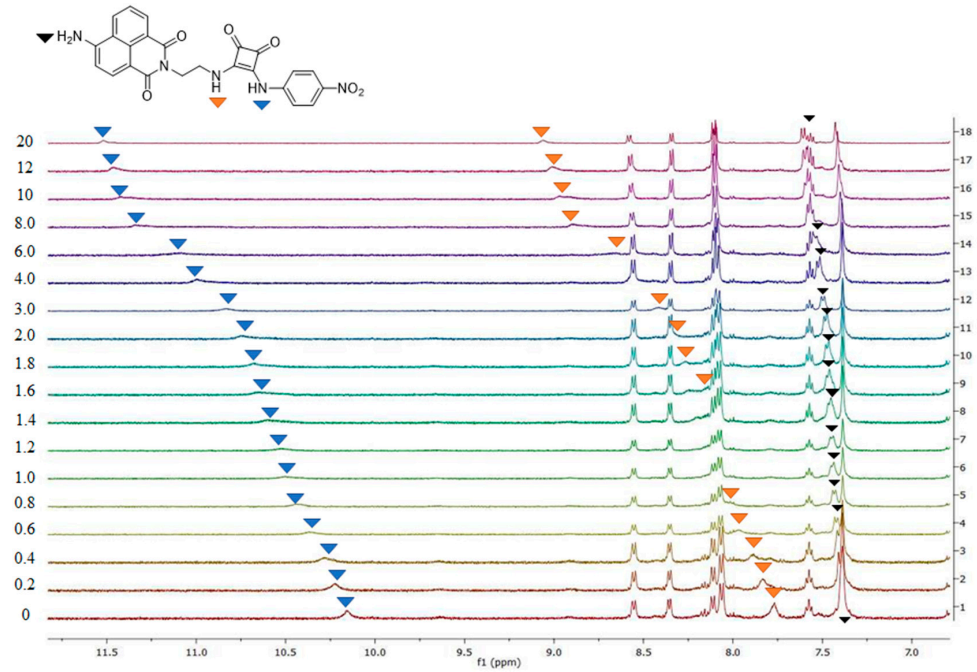

Figure 6. Changes in the ^{1}H NMR spectrum (NH_a, NH_b, NH_c identified) of **SN2** upon the addition 0–20 equivalents of anions as tetrabutylammonium (TBA) chloride in DMSO-d_6.

Overall, both **SN1** and **SN2** were found to bind to Cl^- with moderate affinities, with **SN1** showing a slightly increased affinity compared to **SN2**. As previously reported, the position of the squaramide at the 'tail' of the naphthalimide seems to be optimal for anion binding.

Having observed such stark colour changes while conducting the ^{1}H NMR titrations, we also wished to examine the interaction of **SN1** and **SN2** with anions using UV/Vis spectroscopy. The titrations were performed by additions of aliquots of the putative anionic guest (AcO^-, Cl^-, F^-, HPO_4^{2-}, SO_4^{2-}) as the tetrabutylammonium (TBA) salt solution (20 mM) in DMSO to a 1.2×10^{-5} M solution of the receptor in DMSO. The changes in the UV spectra upon anion addition were monitored for each receptor. The overall changes in the ground state of **SN2** with TBA SO_4^{2-} are shown in Figure 7 as an example.

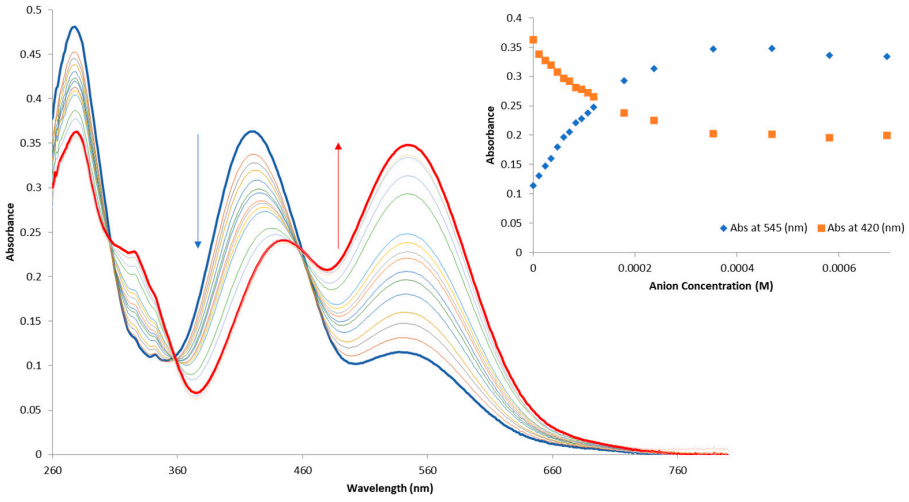

Figure 7. Changes in the UV/Vis spectrum of **SN2** (12 μM) with increasing TBA sulphate concentration in DMSO. Inset: Plot of the change in absorbance at 420 nm (**orange**) and 545 nm (**blue**) as a function of TBA SO_4 concentration.

Upon titration with Cl^-, very minor changes were seen in all cases. In contrast, much more significant changes were seen upon the addition of AcO^-, F^-, HPO_4^{2-}, and SO_4^{2-}. As shown in Figure 5, an increase in absorption at 545 nm was observed with a concomitant decrease at 280 nm and 420 nm and a clear isosbestic point at 460 nm. Similar changes were observed upon titration with AcO^-, F^-, and HPO_4^{2-}. These results again suggest a deprotonation event at the squaramide binding site. The changes in the fluorescence spectra of **SN1** and **SN2** were also monitored, but as expected, only minor changes were observed in the emission spectra of **SN1** and **SN2** upon titration with Cl^-. Titration with AcO^-, F^-, HPO_4^{2-}, and SO_4^{2-} led to more significant changes where some further fluorescence quenching was observed, with a small emission decrease being observed at 430 nm and 460 nm for **SN1** and **SN2**, respectively. We also ascribe this behaviour to the deprotonation observed in the NMR titrations where similar behaviour was also observed in the presence of all basic non-halide anions (see Supplementary Materials). Overall, the results of the anion binding experiments seem to suggest that a moderate H-bonding interaction occurs between Cl^- and both **SN1** and **SN2** but results in very minor spectroscopic perturbation as measured by UV/Vis and fluorescence. Conversely, the interaction of either receptor with more basic anions results in a deprotonation that is accompanied by both stark colour changes as well as further fluorescence quenching.

4. Conclusions

In conclusion, we have reported the synthesis of two new squaramide–naphthalimide conjugates, **SN1** and **SN2**. We have shown that these receptors undergo some degree of self-aggregation in aqueous DMSO as observed by ^{1}H NMR and SEM. We have also shown that both receptors are capable of classical H-bonding to Cl^- and appear to undergo deprotonation in the presence of more basic anions such as AcO^-, F^-, HPO_4^{2-}, and SO_4^{2-}. Deprotonation leads to stark colour changes that are clearly observable to the naked eye and can also be monitored using UV/Vis absorption spectroscopy. Unfortunately, due to the quenching effect of the NO_2 substituent on the 1,8-naphthalimide, large changes in emission characteristics are not observed apart from minor quenching brought about in the presence of basic anions, again, thought to be a result of deprotonation. The position of the squaramide relative to the naphthalimide (i.e., at the head or the tail of the structure) seems to play a role in the strength of the association constant with Cl^-. Under our experimental conditions, **SN1**, which has the squaramide appended to the 'tail' of the naphthalimide, showed a higher affinity when compared to **SN2** where the squaramide is at the 'head' of the naphthalimide. We are currently optimising our design to take advantage of the aggregation–disassembly approach to anion recognition, and our results will be reported in due course.

Supplementary Materials: Supporting information including spectroscopic methods, characterization data, titration data and titration analysis can be downloaded at: https://www.mdpi.com/article/10.3390/chemistry4040085/s1.

Author Contributions: A.A.A., S.A.H. and R.B.P.E. designed the study and wrote the manuscript. R.B.P.E. supervised the study and secured funding for the work. A.A.A. and S.A.H. synthesized and characterized the compounds and carried out spectroscopic titrations and anion binding assays. O.F. conducted Scanning Electron Microscopy experiments. All authors discussed the results and commented on the manuscript. All authors have read and agreed to the published version of the manuscript.

Funding: A.A.A. acknowledges Maynooth University for a University Scholarship. R.E. acknowledges funding from Science Foundation Ireland (SFI), grant number 12/RC/2275/P2, which is co-funded under the European Regional Development Fund. SFI is also acknowledged for the funding of the NMR facility (12/RI/2346/SOF) through the Research Infrastructure Programme and the Advion Compact Mass Spec through the Opportunistic Infrastructure Fund (16/RI/3399).

Data Availability Statement: Not applicable.

Conflicts of Interest: The authors declare no conflict of interest.

References

1. Marchetti, L.A.; Kumawat, L.K.; Mao, N.; Stephens, J.C.; Elmes, R.B.P. The Versatility of Squaramides: From Supramolecular Chemistry to Chemical Biology. *Chem* **2019**, *5*, 1398–1485. [CrossRef]
2. Ian Storer, R.; Aciro, C.; Jones, L.H. Squaramides: Physical properties, synthesis and applications. *Chem. Soc. Rev.* **2011**, *40*, 2330–2346. [CrossRef]
3. Saez Talens, V.; Englebienne, P.; Trinh, T.T.; Noteborn, W.E.M.; Voets, I.K.; Kieltyka, R.E. Aromatic Gain in a Supramolecular Polymer. *Angew. Chem. Int. Ed.* **2015**, *54*, 10502–10506. [CrossRef]
4. Saez Talens, V.; Davis, J.; Wu, C.-H.; Wen, Z.; Lauria, F.; Gupta, K.B.S.S.; Rudge, R.; Boraghi, M.; Hagemeijer, A.; Trinh, T.T.; et al. Thiosquaramide-Based Supramolecular Polymers: Aromaticity Gain in a Switched Mode of Self-Assembly. *J. Am. Chem. Soc.* **2020**, *142*, 19907–19916. [CrossRef]
5. Rostami, A.; Colin, A.; Li, X.Y.; Chudzinski, M.G.; Lough, A.J.; Taylor, M.S. N,N′-Diarylsquaramides: General, High-Yielding Synthesis and Applications in Colorimetric Anion Sensing. *J. Org. Chem.* **2010**, *75*, 3983–3992. [CrossRef]
6. Edwards, S.J.; Valkenier, H.; Busschaert, N.; Gale, P.A.; Davis, A.P. High-Affinity Anion Binding by Steroidal Squaramide Receptors. *Angew. Chem. Int. Ed.* **2015**, *54*, 4592–4596. [CrossRef]
7. Jin, C.; Zhang, M.; Deng, C.; Guan, Y.; Gong, J.; Zhu, D.; Pan, Y.; Jiang, J.; Wang, L. Novel calix[4]arene-based receptors with bis-squaramide moieties for colorimetric sensing of anions via two different interaction modes. *Tet. Lett.* **2013**, *54*, 796–801. [CrossRef]
8. Jagleniec, D.; Siennicka, S.; Dobrzycki, Ł.; Karbarz, M.; Romański, J. Recognition and Extraction of Sodium Chloride by a Squaramide-Based Ion Pair Receptor. *Inorg. Chem.* **2018**, *57*, 12941–12952. [CrossRef]
9. Amendola, V.; Bergamaschi, G.; Boiocchi, M.; Fabbrizzi, L.; Milani, M. The Squaramide versus Urea Contest for Anion Recognition. *Chem. Eur. J.* **2010**, *16*, 4368–4380. [CrossRef]
10. Busschaert, N.; Kirby, I.L.; Young, S.; Coles, S.J.; Horton, P.N.; Light, M.E.; Gale, P.A. Squaramides as Potent Transmembrane Anion Transporters. *Angew. Chem. Int. Ed.* **2012**, *51*, 4426–4430. [CrossRef]
11. Picci, G.; Kubicki, M.; Garau, A.; Lippolis, V.; Mocci, R.; Porcheddu, A.; Quesada, R.; Ricci, P.C.; Scorciapino, M.A.; Caltagirone, C. Simple squaramide receptors for highly efficient anion binding in aqueous media and transmembrane transport. *Chem. Commun.* **2020**, *56*, 11066–11069. [CrossRef]
12. Singh, A.; Torres-Huerta, A.; Vanderlinden, T.; Renier, N.; Martínez-Crespo, L.; Tumanov, N.; Wouters, J.; Bartik, K.; Jabin, I.; Valkenier, H. Calix[6]arenes with halogen bond donor groups as selective and efficient anion transporters. *Chem. Commun.* **2022**, *58*, 6255–6258. [CrossRef]
13. Marchetti, L.A.; Kramer, T.; Elmes, R.B.P. Amidosquaramides-a new anion binding motif with pH sensitive anion transport properties. *Org. Biomol. Chem.* **2022**, *20*, 7056–7066. [CrossRef]
14. Ko, S.-K.; Kim, S.K.; Share, A.; Lynch, V.M.; Park, J.; Namkung, W.; Van Rossom, W.; Busschaert, N.; Gale, P.A.; Sessler, J.L.; et al. Synthetic ion transporters can induce apoptosis by facilitating chloride anion transport into cells. *Nat. Chem.* **2014**, *6*, 885–892. [CrossRef]
15. Busschaert, N.; Park, S.-H.; Baek, K.-H.; Choi, Y.P.; Park, J.; Howe, E.N.W.; Hiscock, J.R.; Karagiannidis, L.E.; Marques, I.; Félix, V.; et al. A synthetic ion transporter that disrupts autophagy and induces apoptosis by perturbing cellular chloride concentrations. *Nat. Chem.* **2017**, *9*, 667–675. [CrossRef]
16. Duke, R.M.; Veale, E.B.; Pfeffer, F.M.; Kruger, P.E.; Gunnlaugsson, T. Colorimetric and fluorescent anion sensors: An overview of recent developments in the use of 1,8-naphthalimide-based chemosensors. *Chem. Soc. Rev.* **2010**, *39*, 3936–3953. [CrossRef]
17. Gunnlaugsson, T.; Davis, A.P.; Glynn, M. Fluorescent photoinduced electron transfer (PET) sensing of anions using charge neutral chemosensors. *Chem. Commun.* **2001**, 2556–2557. [CrossRef]
18. Gunnlaugsson, T.; Davis, A.P.; O'Brien, J.E.; Glynn, M. Synthesis and photophysical evaluation of charge neutral thiourea or urea based fluorescent PET sensors for bis-carboxylates and pyrophosphate. *Org. Biomol. Chem.* **2005**, *3*, 48–56. [CrossRef]
19. Gunnlaugsson, T.; Kruger, P.E.; Jensen, P.; Tierney, J.; Ali, H.D.P.; Hussey, G.M. Colorimetric "naked eye" sensing of anions in aqueous solution. *J. Org. Chem.* **2005**, *70*, 10875–10878. [CrossRef]
20. Pfeffer, F.M.; Buschgens, A.M.; Barnett, N.W.; Gunnlaugsson, T.; Kruger, P.E. 4-Amino-1,8-naphthalimide-based anion receptors: Employing the naphthalimide N-H moiety in the cooperative binding of dihydrogenphosphate. *Tet. Lett.* **2005**, *46*, 6579–6584. [CrossRef]
21. Duke, R.M.; Gunnlaugsson, T. Selective fluorescent PET sensing of fluoride (F-)using naphthalimide-thiourea and -urea conjugates. *Tet. Lett.* **2007**, *48*, 8043–8047. [CrossRef]
22. Parkesh, R.; Lee, T.C.; Gunnlaugsson, T. Highly selective 4-amino-1,8-naphthalimide based fluorescent photoinduced electron transfer (PET) chemosensors for Zn(II) under physiological pH conditions. *Org. Biomol. Chem.* **2007**, *5*, 310–317. [CrossRef]
23. Ali, H.D.P.; Kruger, P.E.; Gunnlaugsson, T. Colorimetric 'naked-eye' and fluorescent sensors for anions based on amidourea functionalised 1,8-naphthalimide structures: Anion recognition via either deprotonation or hydrogen bonding in DMSO. *New J. Chem.* **2008**, *32*, 1153–1161. [CrossRef]

24. Elmes, R.B.P.; Turner, P.; Jolliffe, K.A. Colorimetric and Luminescent Sensors for Chloride: Hydrogen Bonding vs Deprotonation. *Org. Lett.* **2013**, *15*, 5638–5641. [CrossRef]
25. Busschaert, N.; Elmes, R.B.P.; Czech, D.D.; Wu, X.; Kirby, I.L.; Peck, E.M.; Hendzel, K.D.; Shaw, S.K.; Chan, B.; Smith, B.D.; et al. Thiosquaramides: pH switchable anion transporters. *Chem. Sci.* **2014**, *5*, 3617–3626. [CrossRef]
26. Elmes, R.B.P.; Jolliffe, K.A. Amino acid-based squaramides for anion recognition. *Supramol. Chem.* **2014**, *27*, 321–328. [CrossRef]
27. Elmes, R.B.P.; Yuen, K. K.Y. ; Jolliffe, K.A. Sulfate-Selective Recognition by Using Neutral Dipeptide Anion Receptors in Aqueous Solution. *Chem. Eur. J.* **2014**, *20*, 7373–7380. [CrossRef]
28. Elmes, R.B.P.; Busschaert, N.; Czech, D.D.; Gale, P.A.; Jolliffe, K.A. pH switchable anion transport by an oxothiosquaramide. *Chem. Commun.* **2015**, *51*, 10107–10110. [CrossRef]
29. Qin, L.; Hartley, A.; Turner, P.; Elmes, R.B.P.; Jolliffe, K.A. Macrocyclic squaramides: Anion receptors with high sulfate binding affinity and selectivity in aqueous media. *Chem. Sci.* **2016**, *7*, 4563–4572. [CrossRef]
30. Marchetti, L.A.; Mao, N.; Krämer, T.; Kitchen, J.A.; Elmes, R.B.P. A long wavelength colourimetric chemosensor for fluoride. *Supramol. Chem.* **2018**, *30*, 795–805. [CrossRef]
31. Masilamani, G.; Batchu, H.; Amsallem, D.; Bedi, A. Novel Series of Diaminoanthraquinone-Based π-Extendable Building Blocks with Tunable Optoelectronic Properties. *ACS Omega* **2022**, *7*, 25874–25880. [CrossRef] [PubMed]
32. Kumawat, L.K.; Abogunrin, A.A.; Kickham, M.; Pardeshi, J.; Fenelon, O.; Schroeder, M.; Elmes, R.B.P. Squaramide—Naphthalimide Conjugates as "Turn-On" Fluorescent Sensors for Bromide Through an Aggregation-Disaggregation Approach. *Front. Chem.* **2019**, *7*, 354. [CrossRef] [PubMed]
33. Liu, H.; Tomooka, C.S.; Moore, H.W. An Efficient General Synthesis of Squarate Esters. *Synth. Commun.* **1997**, *27*, 2177–2180. [CrossRef]
34. Roke, D.; Wezenberg, S.J.; Feringa, B.L. Molecular rotary motors: Unidirectional motion around double bonds. *Proc. Natl. Acad. Sci. USA* **2018**, *115*, 9423–9431. [CrossRef]
35. Cao, X.; Meng, L.; Li, Z.; Mao, Y.; Lan, H.; Chen, L.; Fan, Y.; Yi, T. Large Red-Shifted Fluorescent Emission via Intermolecular π–π Stacking in 4-Ethynyl-1,8-naphthalimide-Based Supramolecular Assemblies. *Langmuir* **2014**, *30*, 11753–11760. [CrossRef]
36. Collado-Fregoso, E.; Zugazagoitia, J.S.; Plaza-Medina, E.F.; Peon, J. Excited-State Dynamics of Nitrated Push−Pull Molecules: The Importance of the Relative Energy of the Singlet and Triplet Manifolds. *J. Phys. Chem. A* **2009**, *113*, 13498–13508. [CrossRef]
37. Adair, L.D.; Trinh, N.; Vérité, P.M.; Jacquemin, D.; Jolliffe, K.A.; New, E.J. Synthesis of Nitro-Aryl Functionalised 4-Amino-1,8-Naphthalimides and Their Evaluation as Fluorescent Hypoxia Sensors. *Chem. Eur. J.* **2020**, *26*, 10064–10071. [CrossRef]
38. Jin, C.; Zhang, M.; Wu, L.; Guan, Y.; Pan, Y.; Jiang, J.; Lin, C.; Wang, L. Squaramide-based tripodal receptors for selective recognition of sulfate anion. *Chem. Commun.* **2013**, *49*, 2025–2027. [CrossRef]
39. Prohens, R.; Tomàs, S.; Morey, J.; Deyà, P.M.; Ballester, P.; Costa, A. Squaramido-based receptors: Molecular recognition of carboxylate anions in highly competitive media. *Tet. Lett.* **1998**, *39*, 1063–1066. [CrossRef]
40. Prohens, R.; Martorell, G.; Ballester, P.; Costa, A. A squaramide fluorescent ensemble for monitoring sulfate in water. *Chem. Commun.* **2001**, 1456–1457. [CrossRef]
41. Piña, M.N.; Soberats, B.; Rotger, C.; Ballester, P.; Deyà, P.M.; Costa, A. Selective sensing of competitive anions by non-selective hosts: The case of sulfate and phosphate in water. *New J. Chem.* **2008**, *32*, 1919–1923. [CrossRef]
42. Delgado-Pinar, E.; Rotger, C.; Costa, A.; Pina, M.N.; Jimenez, H.R.; Alarcon, J.; Garcia-Espana, E. Grafted squaramide monoamine nanoparticles as simple systems for sulfate recognition in pure water. *Chem. Commun.* **2012**, *48*, 2609–2611. [CrossRef] [PubMed]
43. Brynn Hibbert, D.; Thordarson, P. The death of the Job plot, transparency, open science and online tools, uncertainty estimation methods and other developments in supramolecular chemistry data analysis. *Chem. Commun.* **2016**, *52*, 12792–12805. [CrossRef] [PubMed]
44. Thordarson, P. Determining association constants from titration experiments in supramolecular chemistry. *Chem. Soc. Rev.* **2011**, *40*, 1305–1323. [CrossRef] [PubMed]
45. Lowe, A.J.; Pfeffer, F.M.; Thordarson, P. Determining binding constants from 1H NMR titration data using global and local methods: A case study using [n]polynorbornane-based anion hosts. *Supramol. Chem.* **2012**, *24*, 585–594. [CrossRef]